

## 16D.4 DIURNA VARIATIONS OF THE WATER CYCLE IN THE GODDARD MULTI\_SCALE MODELING FRAMEWORK

Jiun-Dar Chern<sup>\*,1,2</sup>, Wei-Kuo Tao<sup>1</sup>, and Xin Lin<sup>1,2</sup>

<sup>1</sup>Laboratory for Atmospheres, NASA/Goddard Space Flight Center, Greenbelt, MD 20771

<sup>2</sup>Goddard Earth Sciences and Technology Center, University of Maryland Baltimore County, Baltimore, MD 21250

### 1. INTRODUCTION

One of the major uncertainties in climate and climate change modeling is the representation of sub-grid cloud processes in the General Circulations Models (GCMs). Recently, the Multi-scale Modeling Framework (MMF) [or a super parameterization], which replaces the conventional cloud parameterizations with a Cloud Resolving Model (CRM) in each grid column of a GCM, constitutes an innovative and promising approach to break the deadlock of conventional cloud parameterizations in GCMs (Grabowski and Smolarkiewicz 1999, Randall et al. 2003, Khairoutdinov et al. 2005). The MMF can explicitly simulate the sub-grid cloud-scale processes and their interactions with radiation, aerosol, and surface processes at the resolution of a CRM. It also provides for global coverage, and two-way interactions between CRMs and their parent GCM. Recently, a Goddard MMF has been successfully developed based on a 2D version of the Goddard Cumulus Ensemble (GCE) model and the Goddard finite volume GCM (fvGCM) model. The major objectives of our research are to: (1) to use NASA satellite data and field campaign observations for validating and improving the MMF; (2) to compare the MMF results with results from conventional GCMs and other MMFs; (3) to produce and provide multi-dimensional cloud datasets (i.e., a cloud data library) to the global modeling community to help improve the representation of moist processes in climate models and to improve our understandings of cloud and radiation processes.

To fully understand the strengths and weakness of the MMF approach in climate modeling, more research is needed to systematically study the MMF modeling system and the offline 2D and 3D CRM simulations. The model results also need to

be tested thoroughly and rigorously against observations. The diurnal cycle is a fundamental mode of atmospheric variability. It has a major impact on weather and climate prediction. In addition, it also provides a robust test of physical processes represented in atmospheric models that are used for studying the water/energy cycle. Most current GCMs can simulate the diurnal cycle of clouds and precipitation to some extent. But, the biggest difficulty in most GCMs is in the simulated phase and amplitude of the diurnal cycle (i.e., Yang and Slingo 2001, Dai and Trenberth 2004 and many others). In this study the diurnal variations of clouds and precipitation in the MMF will be evaluated against the fvGCM simulations and satellite observations.

### 2. MODEL

The Goddard is based on a 2D version of the Goddard Cumulus Ensemble (GCE) model and the Goddard finite volume GCM (fvGCM) model. The GCE model, a CRM, has been developed and improved at NASA Goddard Space Flight Center over the past two decades. The development and main features of the GCE model were published in Tao and Simpson (1993) and Tao *et al.* (2003). A review of the applications of the GCE model to develop a better understanding of precipitation processes can be found in Simpson and Tao (1993) and Tao (2003). The 2D version of the GCE model is typically run using 512 x 43 up to 1024 x 43 grid points at 1-2 km resolution or better. The fvGCM has been constructed with the unique finite-volume dynamic core developed at Goddard (Lin 2004) and the physics package from the NCAR Community Climate Model CCM3, which represents a well-balanced set of processes with a long history of development and documentation (Kiehl *et al.* 1998). The unique features of the finite-volume dynamical core include: an accurate conservative flux-form semi-Lagrangian transport algorithm (FFSL) with a monotonicity constraint on sub-grid distribution that is free of Gibbs oscillation (Lin and Rood 1996, 1997), a terrain-following Lagrangian

---

\*Corresponding author address: Dr. Jiun-Dar Chern, Code 613.1, NASA/GSFC, Greenbelt, MD 20771; email: jchern@agnes.gsfc.nasa.gov

control-volume vertical coordinate, a physically consistent integration of pressure gradient force for a terrain-following coordinate (Lin 1997, 1998), and a mass, momentum, and total energy conserving mapping algorithm for Lagrangian to Eulerian control-volume vertical coordinate transformation. The physical parameterizations in the fvGCM have been upgraded with the gravity wave scheme from the NCAR Whole Atmosphere Community Model (WACCM) and the CLM version 2 (CLM-2).

Because the MMF approach is extremely computer demanding, a simple framework has been developed first and used as much as possible to explore its capabilities and limitations. The Goddard MMF includes the fvGCM run at  $2.5^\circ \times 2^\circ$  horizontal resolution with 32 vertical layers from the surface to 0.4 hpa and the 2D GCE using 64 horizontal and 28 vertical grid points with 4 km horizontal resolution and cyclic lateral boundaries. Globally, there are a total of 13,104 GCEs running at the same time. The time step for the 2D GCE is 10 seconds, and the fvGCM-GCE coupling frequency is one hour (i.e., the fvGCM physical time step). At each fvGCM column, the global model provides the mean atmospheric conditions and the large-scale temperature and moisture advection forcings to the GCE and the cloud model feedbacks the tendencies of thermodynamic variables and cloud statistics. As the vertical coordinate of the fvGCM (a terrain-following coordinate) is different from that of the GCE (a z coordinate), vertical interpolations between the two coordinates are needed in the coupling interface. A new finite-volume piecewise parabolic mapping (PPM) algorithm, which conserves the mass, momentum and moist static energy in the z coordinate is being developed to interpolate fields from the fvGCM to the GCE.

### 3. RESULTS

The MMF system has been applied and its performance tested for two different climate scenarios, El Nino (1998) and La Nina (1999). The initial conditions for two yearly simulations come from  $1^\circ \times 1.25^\circ$  Goddard GEOS4 analysis at 0000 UTC 1 November 1997 and 1998, respectively. The experiments are run with observed NOAA weekly OI SST in a climate free run mode. A similar run with the same initial conditions and SSTs was performed using the fvGCM with convective parameterizations to help identify common deficiencies in the GCMs. Figure 1 shows the geographical distribution of simulated seasonal mean precipitation in winter and summer

1998 and 1999 from the MMF and fvGCM along with the corresponding observations from the  $0.5^\circ \times 0.5^\circ$  TRMM TMI product. In general, the observed precipitation pattern is well reproduced by the MMF for both extra-tropical storm tracks and the Tropics. The shift in tropical precipitation to the central Pacific in winter 1998 during the El Nino period is well simulated. The inter-tropical convergence zone (ITCZ), the South Pacific convergence zone (SPCZ), and the South Atlantic convergence zone (SACZ) are also well reproduced. The MMF precipitation patterns and dry areas are superior to those of the fvGCM. The MMF results do not have the double ITCZ problem that is very common in most GCMs. There are apparent biases in the MMF however; the mean precipitation over the Tropics is more than the TRMM observations in both winter and summer. The MMF precipitation in the western Pacific, eastern tropical Pacific, Bay of Bengal and western India Ocean is too high in summer. Even without any tuning of the MMF, the simulated total precipitable water and the earth's radiation budget are at least comparable in quality to those of the fvGCM. Figure 2 shows the observed seasonal mean total precipitable water from NASA water vapor project (NVAP) and simulations from the fvGCM and the MMF in winter and summer 1998. The total column water vapor at ITCZ, SPCZ, and SACZ is well reproduced. The increase of total precipitable water in central Pacific during the El Nino is also well simulated. Figure 3 shows the seasonal mean high cloud amount of the ISCCP D2 observation and simulations from the fvGCM and the MMF for the winter and summer season of 1998. Compared with the ISCCP data, the large biases of high cloud amount in the fvGCM are significantly reduced in the MMF simulations.

To fully evaluate the performance of the MMF approach in climate modeling, we need to examine not only the simulated mean climate but also its capability in simulating the low and high frequency of climate variation. The Hovmoller diagrams for the precipitation rate in the tropic ( $10^\circ \text{S} - 10^\circ \text{N}$ ) for 1998 and 1999 (not shown here) indicate that the MMF is superior to the fvGCM in producing one of the most important low frequency variation in the tropic-the Madden-Julian oscillation (MJO) signal. The MMF produces a vigorous MJO in contrast to the fvGCM run where the MJO is virtually nonexistent. The simulated MJO obtained with the MMF has more realistic propagation speed and direction. The simulated changes due to El Nino (1998) and La Nina (1999) are also consistent with observations

The diurnal cycle is a fundamental mode of atmospheric high frequency variability. It has a major impact on weather and climate prediction. In addition, it also provides a robust test of physical processes represented in climate models. Figure 4 (not shown) shows the geographical distribution of the local solar time (LST) of the non-drizzle precipitation frequency maximum for the winter (left panels) and summer (right panels) of 1998 as simulated with the Goddard MMF (top panels) and the fvGCM (middle panels) and as observed by satellite from 1998-2005 (bottom panels). The results show that the MMF is superior to the fvGCM in reproducing the correct timing of the frequency maximum in late afternoon (1400-1600 LST) over land and in early morning (0500-0700 LST) over ocean. The phases and amplitudes of the diurnal cycle of precipitation rate are computed using a harmonic analysis. Figure 5 shows the phase and amplitudes of the diurnal cycle of precipitation in South America. It is clear that there is some systematic geographical variation. For example, over Amazon region, the preferred times of precipitation tend to be in the afternoon in the MMF simulation and in the late morning in the fvGCM simulation.

#### 4. SUMMARY

Recently, a Goddard MMF has been successfully developed based on a 2D version of the Goddard Cumulus Ensemble (GCE) model and the Goddard finite volume GCM (fvGCM) model. Two yearly MMF integrations for 1998 (El Nino) and 1999 (La Nina) have been carried out on NASA Columbia supercomputer. The preliminary results are compared with the results from fvGCM AMIP run, and satellite observations to evaluate the MMF performances. It is shown that the MMF is superior to the fvGCM in producing mean climate, low frequency variation and diurnal cycle. The MMF is a promising approach for climate modeling and has a great potential to substantially reduce systematic errors in GCMs.

#### REFERENCES

Dai, A., and K.E. Trenberth, 2004: The diurnal cycle and its depiction on the community climate system model. *J. Climate*, **17**, 930-951.  
 Grabowski, W. W., and P. K. Smolarkiewicz, 1999: CRCP: A cloud resolving convective parameterization for modeling the tropical convective atmosphere. *Physica D*, **133**, 171-178.

Kiehl, J. T., J. J. Hack, G. B. Bonan, B. A. Boville, D. L. Williamson, and P. J. Rasch, 1998: The National Center for Atmospheric Research Community Climate Model: CCM3. *J. Climate*, **11**, 1131-1150.  
 Khairoutdinov, M. F., D. A. Randall, and C. DeMott, 2005: Simulations of the atmospheric general circulation using a cloud-resolving model as a superparameterization of physical processes. *J. Atmos. Sci.*, **62**, 2136-2154.  
 Lin, S.-J., 1997: A finite-volume integration method for computing pressure gradient forces in general vertical coordinates. *Q. J. Roy. Met. Soc.*, **123**, 1749-1762.  
 Lin, S.-J., 1998: Reply to comments by T. Janjic on "A finite-volume integration method for computing pressure gradient forces in general terrain-following coordinates". *Q. J. Roy. Met. Soc.*, **124**, 1749-1762.  
 Lin, S.-J., 2004: A "vertically Lagrangian" finite-volume dynamical core for global models. *Mon. Wea. Rev.*, **32**, 2293-2307.  
 Lin, S.-J., and R. B. Rood, 1996: Multidimensional flux-form semi-Lagrangian transport schemes. *Mon. Wea. Rev.*, **124**, 2046-2070.  
 Lin, S.-J., and R. B. Rood, 1997: An explicit flux-form semi-Lagrangian shallow water model on the sphere. *Q. J. Roy. Met. Soc.*, **123**, 2477-2498  
 Randall, D., M. Khairoutdinov, A. Arakawa, and W. Grabowski, 2003b: Breaking the cloud parameterization deadlock. *B. Amer. Meteor. Soc.*, **84**, 1547-1564.  
 Tao, W.-K., 2003: Goddard Cumulus Ensemble (GCE) model: Application for understanding precipitation processes, *AMS Monographs - Cloud Systems, Hurricanes and TRMM*. 103-138  
 Tao, W.-K., and J. Simpson, 1993: The Goddard Cumulus Ensemble Model. Part I: Model description. *Terrestrial, Atmospheric and Oceanic Sciences*, **4**, 19-54.  
 Tao, W.-K., J. Simpson, D. Baker, S. Braun, D. Johnson, B. Ferrier, A. Khain, S. Lang, C.-L. Shie, D. Starr, C.-H. Sui, Y. Wang and P. Wetzel, 2003: Microphysics, Radiation and Surface Processes in a Non-hydrostatic Model, *Meteorology and Atmospheric Physics*, **82**, 97-137.

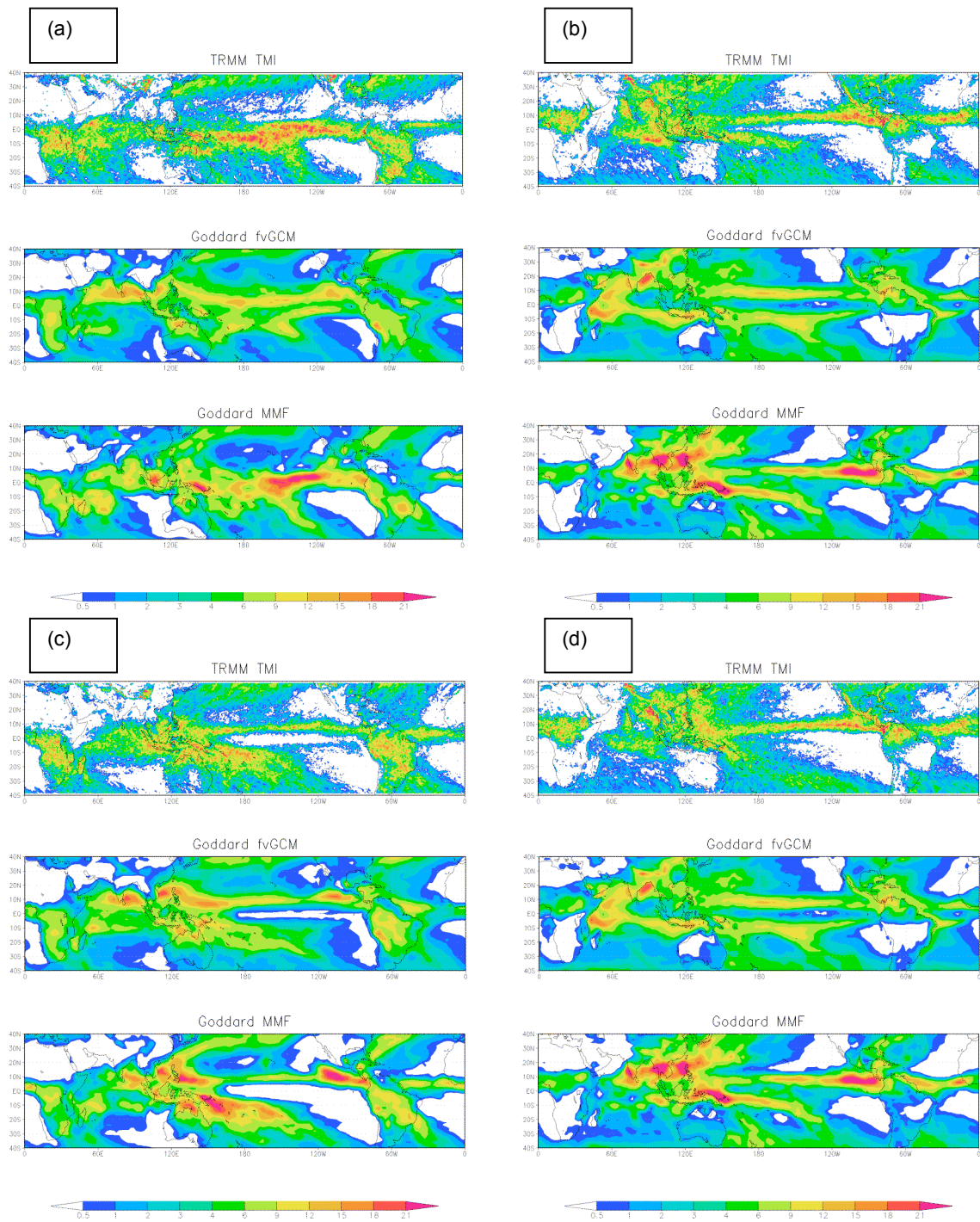


Figure 1. Seasonal mean precipitation rate (mm/day) from the TRMM/TMI (top panels) and simulated from the fvGCM (middle panel) and the Goddard MMF (bottom panel) for (a) winter 1998, (b) summer 1998, (c) winter 1999, and (d) summer 1999.

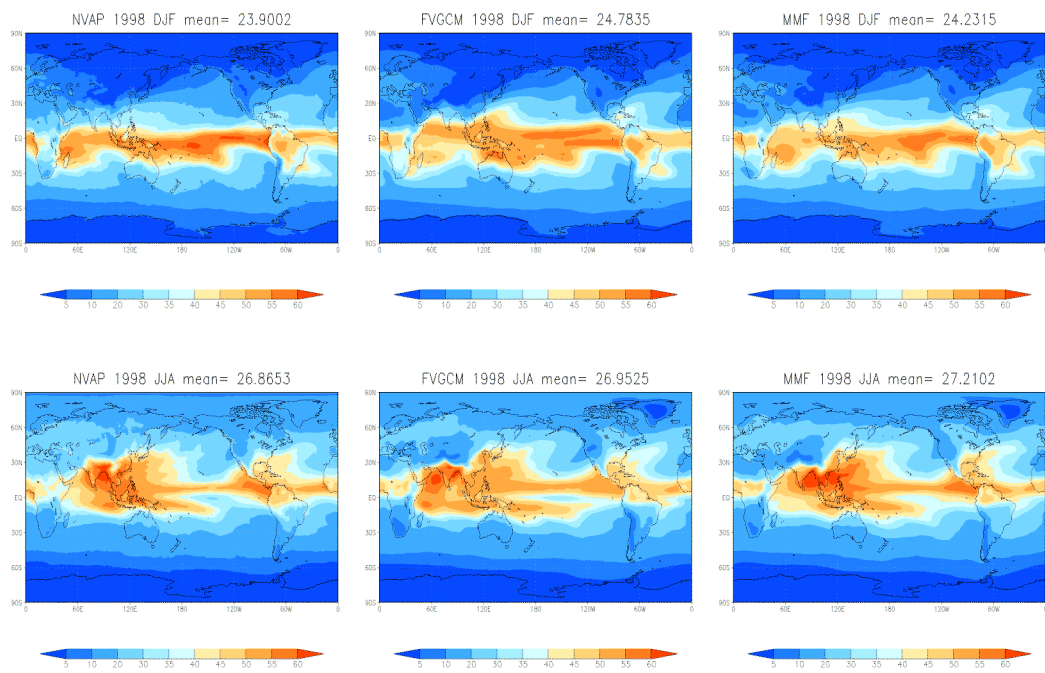


Figure 2. Seasonal mean total precipitable water (mm) from the NVAP (left panels) and simulated from the fvGCM (center panel) and the Goddard MMF (right panel) for winter (top panels) and summer (lower panels) 1998.

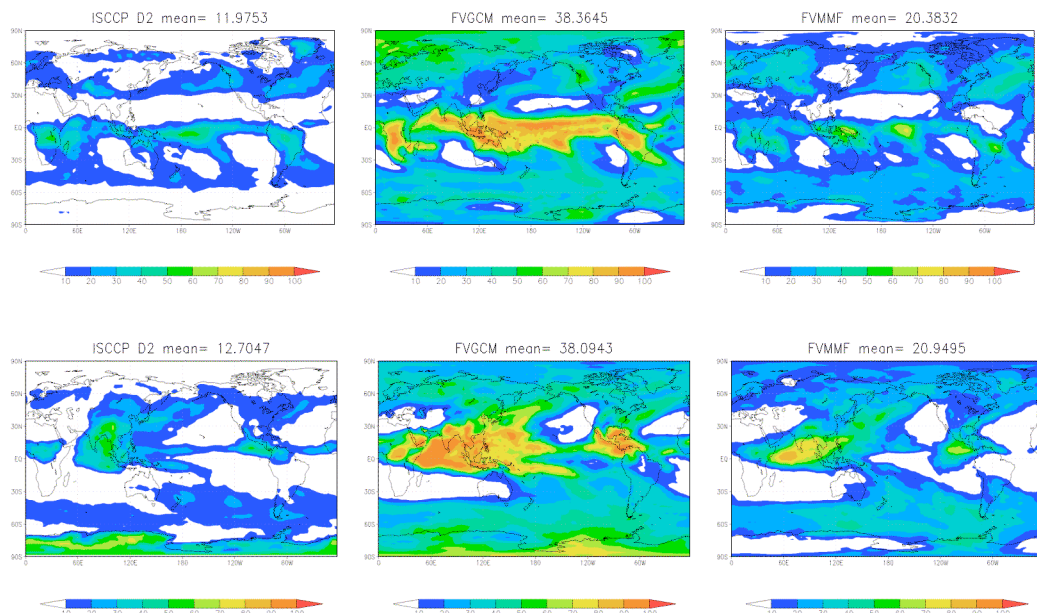


Figure 3. Seasonal mean high cloud amount (%) from the ISCCP D2 observation (left panels) and simulated from the fvGCM (center panel) and the Goddard MMF (right panel) for winter (top panels) and summer (lower panels) 1998.

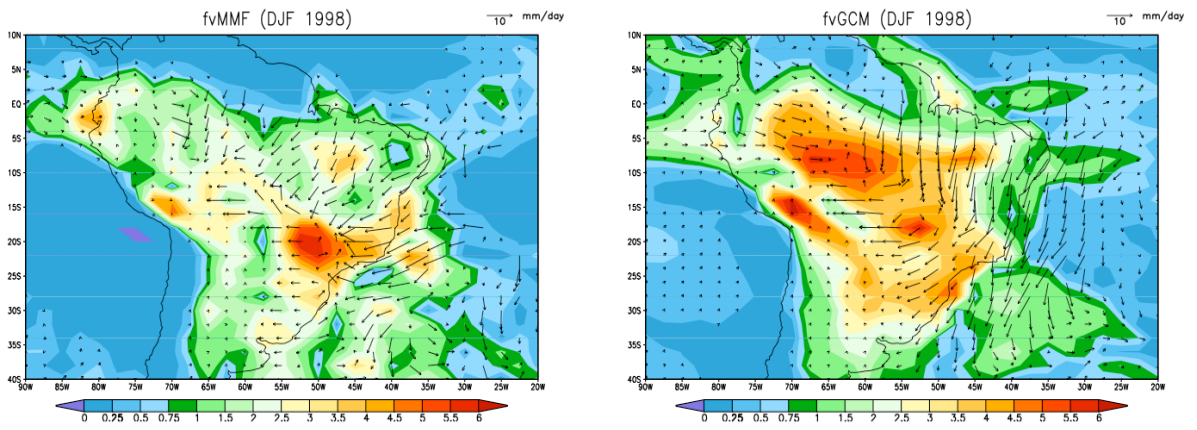


Figure 5. Diurnal variations of mean rain rate for winter 1988 simulated from the MMF (right panel) and the fvGCM (left panel). Lengths of arrows and color plot represent the mean diurnal amplitudes and direction of arrows represent preferred local times of precipitation.